WATER EXCHANGE OF A STANDING COLUMN WELL WITH AQUIFER
A Numerical Study

by

Long NI[a,*], Rong WANG[a], Xianjing SUN[b], Yang YAO[a], and Dehu QV[a,c]

[a] School of Architecture, Harbin Institute of Technology, Harbin, China
[b]Central-South Architectural Design Institute Co., Ltd., Wuhan, China
[c] Guangdong Jirong Air-Conditioning Co., Ltd., Guangdong, China

Original scientific paper
https://doi.org/10.2298/TSCI171011260N

Part of groundwater circulating in the well conduct mass exchange with the aquifer. This part of exchange (the raw water exchange) is indicated the groundwater flow and heat transfer in a typical standing column well. In order to study the water exchange between the standing column well and the aquifer quantitatively, a mathematic model of flow in a standing column well and coupled heat transfer of well pipe, well hole and aquifer was developed. The model was verified by the field test of a standing column well, and results show that the simulated temperature values of drawing water were in good agreement with the measured values both in the cooling and heating condition with the deviation less than 10% and the correlation coefficient up to 0.998. The raw water exchange of a standing column well was studied quantitatively by defining the raw water exchange ratio and the raw water exchange load ratio. For the typical example, the exchange ratio of raw water and the load ratio by raw water exchange were almost constant with the data of 29.6% and 23.4%, respectively.

Key words: *standing column well, raw water exchange, heat transfer, mathematic model*

Introduction

The ground source heat pump (GSHP) system which utilizes the almost constant underground temperature that not affected by the seasons as the source of a heat pump or refrigerator. Among the GSHP system, the standing column well (SCW) has better heat transfer performance than other soil heat exchangers [1], it also needs less well depth to get per kW heat [2]. Sometimes, the abandoned geothermal wells can be utilized [3].

In 1986, the first literal SCW was proposed by Tan and Kush [4], by removing PVC jacket to let drawing and returning water transfer heat with the bedrock directly. From 1993 to 1995, Yuill and Mikler [1] did related research on the SCW proposed by Tan and Kush [4]. They established a simple and 1-D coupled flow and heat transfer model, and the groundwater flow in the aquifer was analyzed using the *equivalent heat transfer coefficient*. Woods and Ortega [5] established the finite linear heat source model, and obtained the instantaneous solu-

* Corresponding author, e-mail: nilonggn@163.com; qdh000@126.com

tion, short time solution and long time analytical solution. Choi *et al*. [6] and Lee *et al*. [7] utilized the linear heat source theory to establish the response model for thermal properties test of SCW. Due to groundwater flow, when permeability coefficient of the rock is greater than 1E-08 m/s, the thermal response test is not suitable for SCW [8].

In the previous models, researchers all consider that the underground water flows in the well entirely, without considering the mass exchange through the wall of well. However, the field test [1] results show that the raw water underground enters the well and participates in the circulation during the operation of the system. Nguyen *et al*. [9] established a numerical coupled ODE model for SCW shows that temperature differences between the homogeneous and fractured aquifer were particularly important when the well was operated at typical bleed ratios.

In fact, a SCW is directly a well hole in the bedrock layer, part of groundwater is circulating in the well bore and exchanges heat with the rock of the well wall, the other part flows into and out of the well exchanging mass with the aquifer. The mass exchange of groundwater between the aquifer and the well enhanced the heat transfer ability of the SCW obviously. To solve this complex and coupled groundwater flow problem, a mathematic model of multi-regime groundwater flow and a heat transfer model of well pipe, well wall and aquifer are established. By numerical solution, water exchange between the SCW and the aquifer is analyzed in detail and studied quantitatively.

Mathematic model and validation

Mathematic model

Mathematic model of multi-regime flow

A SCW can be considered as deformation of the tube heat exchanger of the GSHP. The casing pipe, drawing water from the bottom of the well through the suction pipe, discharging groundwater to the upper part of the well after heat exchange.

In order to simplify the mathematic model, the following hypotheses are put forward:

- The aquifer is an artesian aquifer.
- In the anisotropic aquifer, the main permeability direction is the same as the direction of the co-ordinate axis, and the production of each sub layer in heterogeneous aquifer is horizontal.
- The influence of temperature on permeability coefficient, coefficient of water storage, and density of the groundwater are ignored.
- The influence of solid particle migration on porosity and permeability coefficient of the aquifer are ignored [10].

Groundwater flow in the well hole is influenced by the drawing water of the suction pipe and the returning water in the upperpart of the well hole. Therefore, pipe flow inside the suction pipe, pipe flow with seepage in the well hole and seepage flow in the aquifer need to be solved simultaneously. The schematic diagram of the flow model is shown in fig. 1.

Pipe flow and seepage flow are two different forms of flow with different governing equations. From the perspective of flow energy, governing equation of the pipe flow is the energy loss (Weisbach-Darcy) equation, while control equation of the seepage flow is Darcy law [11]. The model does not take the loss causing by local resistance into account, which is called well loss because the flow rate changes per unit of well deep is very small, so the well loss is neglected in this paper.

Coupled heat transfer model

Effective thermal conductivity of the aquifer is composed of two parts: stagnant thermal conductivity of the aquifer when groundwater does not flow, and thermal dispersion. From the pore scale, heat transfer description of the aquifer includes the local energy conservation equation of the liquid and solid phase, and the Navier-Stokes equation of the liquid phase [12]. Because of the existence of solid skeleton, the magnitude and orientation of the pore velocity changes all the time. Thermal dispersion [13] is needed to be considered in the thermal equilibrium equation. Heat transfer caused by the thermal dispersion effect may be very large, especially near the wall of well [14].

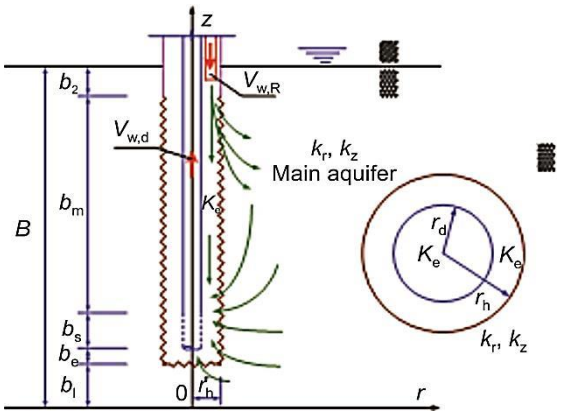

Figure. 1 Schematic diagram of the water flow model

Establish the energy conservation equation of solid skeleton and the fluid in the porous media, respectively. Then merge the energy conservation equations of the solid skeleton and the fluid together utilizing the local thermal equilibrium assumption, finally, get the energy conservation equation of heat transfer in the aquifer as the eq. (1) shows:

$$C\frac{\partial T}{\partial t}+\frac{1}{r}\frac{\partial}{\partial r}\left(rC_{\mathrm{w}}Tq_{\mathrm{r}}\right)+\frac{\partial}{\partial z}\left(C_{\mathrm{w}}Tq_{\mathrm{z}}\right)=\frac{1}{r}\frac{\partial}{\partial r}\left(rk_{\mathrm{r}}\frac{\partial T}{\partial r}\right)+\frac{\partial}{\partial z}\left(k_{\mathrm{z}}\frac{\partial T}{\partial z}\right) \tag{1}$$

where T is the temperature of the aquifer, the roof, and bottom rock layer, C – the volumetric heat capacity of the aquifer, the roof, and bottom rock layer, C_{w} – the volumetric heat capacity of groundwater, k_{r}, k_{z} – the effective thermal conductivity of the aquifer and the thermal conductivity of roof and bottom rock layer, respectively, q_{r}, q_{z} – the seepage velocity of groundwater, and 0 for the roof and bottom rock layer, and r, z – represents the horizontal and vertical direction.

For energy storage of the aquifer, it is generally considered that thermal dispersion is proportional to $|q|^m$ $(m=1,2)$, and m = 1 is more commonly used:

$$k_{\mathrm{A}}=k_{\mathrm{a}}+\alpha C_{\mathrm{w}}|q| \tag{2}$$

where k_{a} is the stagnation thermal conductivity of the aquifer, α – the thermal dispersion, and q – the seepage velocity of groundwater.

The heat exchange sketch maps of well pipe and well hole are shown in fig. 2. In the heat transfer model of well hole and well pipe, the energy conservation equation of the well wall is not included. Heat exchange between the returning pipe and the well hole is not considered in the model. The thermal resistance of the well wall is considered while ignoring the heat capacity of it.

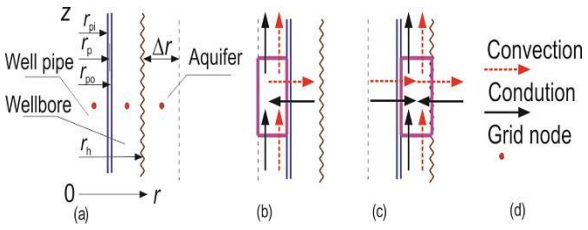

Figure 2. Sketch maps of the heat transfer in the drawing pipe, well hole, and well pipe; (a) size sample, (b) well pipe, (c) wellbore, (d) legend

Model solution

The control equations are discretized by fully implicit and finite volume method, and for the convective term, the discretization scheme is QUICK. Boundary conditions and source terms are handled by additional source term method, the harmonic average method is used to deal with the interface parameters, nodes are set-up by the internal node method, and the grids are structured and asymmetric [11]. Applying MATLAB 7.1 (R14) to the program. The solution accuracy of the flow equation and the temperature field is 10^{-7} m and 10^{-5} °C, respectively.

Model validation

The experimental data of the first 30 days is used for parameter identification, and the subsequent data is used for model validation. Considering that the influence of heat transfer in the horizontal direction is much smaller, the dimensions of the model verification and simulation range were illustrated in tab. 1. A symmetrical mesh method is adopted, and the grids are concentrated close to the axis of the shaft. Time step is set to 2 hours.

Table 1. The dimensions of the model verification and simulation range

	Dimensions, [m]	
	Horizontal	Vertical
Model verification	2000	345
Simulation range	100	360

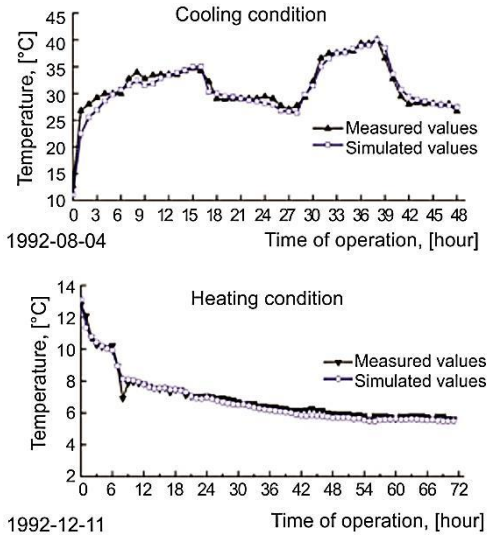

Figure 3. Comparison of drawing water temperature between the simulation and experiment

The simulated and measured values of the drawing water temperature under cooling and heating conditions are shown in fig. 3. We can know that simulated values are in good agreement with measured values under both cooling and heating conditions, and the simulated values track the change of the measured values completely. In the initial stage of the cooling condition, the error is relatively large, and in the latter stage, the error is smaller. Under the heating condition, the simulation results are in better agreement with the measured values due to the small load change. In addition to individual points, the simulated values are all within 10% error limits. The statistical results show that, when the drawing water temperature variation is up to 35.0 °C, the mean error is only 0.5 °C, the mean square deviation is 0.07 °C, the standardized mean square deviation is 1.8%, and the correlation coefficient is 0.998. This shows that the mathematic model of groundwater flow and heat transfer in a SCW is feasible and reliable. The properties of the aquifer are shown in tab. 2.

Results and analysis

Numerical simulation of groundwater flow and heat transfer in a typical SCW is carried out previously using the Mathematic model above. The SCW supplies heat for a one-floor office building in Beijing, construction area of the building is 1020 m^2, thermal parame-

Table 2. Properties of the aquifer

	Aquifer	Upper insulation layer	Lower insulation layer
Permeability coefficient, [ms^{-1}]	$1.0\cdot10^{-5}$	–	–
Water storage coefficient, [m^{-1}]	$1.0\cdot10^{-6}$	–	–
Specific volume heat capacity, [kJm^{-3}°C^{-1}]	2700	2600	2740
Thermal conductivity, [Wm^{-1}°C^{-1}]	3.0	2.5	2.5
Thermal dispersion tensor, [m]	0.35	–	–

ters of the building envelope meet the *Design standard for energy efficiency of public buildings /GB 50189-2015*. Simulation in DeST shows that the heating period is November 8 to March 2, total for 115 days, and the design heating load is 88 kW. According to the performance curve of the actual heat pump unit, hourly heating load of the SCW is shown in fig. 4, and the maximum heating load is 69 kW, the accumulated heating load during the heating season is 316 GJ.

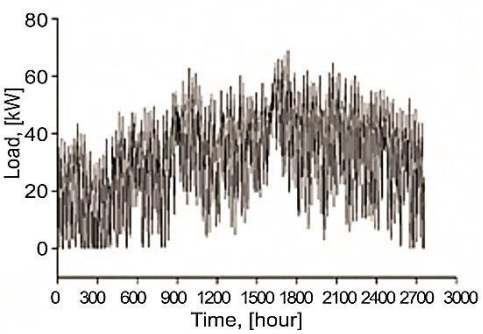

Figure 4. Hourly load of heat source/sink well of P-BJ1

The Custer limestone aquifer is taken as the typical aquifer without leakage. The aquifer is isotropic, and parameters of the aquifer are listed in tab. 3. The structure parameters and physical parameters of the SCW are mostly from the widely used well [15] in the United States as shown in tab. 4.

Table 3. Parameters of the aquifer

Parameter	Unit	Value
Drawing water flow rate	m^{3}h^{-1}	12
Discharging water flow rate	m^{3}h^{-1}	12
Depth	m	30
Thickness	m	300
Permeability coefficient	ms^{-1}	$2\cdot10^{-5}$
Water storage coefficient	m^{-1}	$1\cdot10^{-6}$
Specific volume heat capacity	kJm^{-3}°C^{-1}	2600
Thermal conductivity	Wm^{-1}°C^{-1}	2.5
Thermal dispersion tensor	m	1
Initial temperature	°C	13
Temperature gradient of the ground	°Cm^{-1}	0.01
Depth of the constant temperature layer	m	30

Table 4. Properties and dimensions of the SCW

Items	Depth	Diameter	Wall thickness	Roughness	Thermal conductivity
	m	mm	mm	mm	Wm^{-1}°C^{-1}
Well hole	320	152.4	-	1.5	-
Drawing pipe	318	101.6	6.35	0.01*	0.10
Returning pipe	2	33.4	3.05	-	4.00

* Common values from PVC tube

Phenomenon of raw water exchange

Figure 5 shows the equal drawdown of the aquifer after 10 hours operation of the heat pump. As can be seen from fig. 5, drawdown of the upper part is negative, indicating that the returning water in the well hole flows into the aquifer, and generates re-circulation effect. Drawdown of the lower part is positive, indicating that water flows from the aquifer into well hole, and generates drawing effect. That is to say, there is groundwater exchange between the well hole and aquifer, and this is a remarkable characteristic of the SCW compared with the heat exchanger of the GSHP. However, absolute value of the drawdown is very small, demonstrating that water exchange between the well hole and the aquifer is not large, most of the groundwater circulates in the well hole.

Figure 6 shows the change of the absolute value of the velocity with depth, including the vertical velocity in the well hole and the horizontal velocity of the first node in the aquifer (r = 0.0934 m, 0.0172 m from the wall of the well). As can be seen from fig. 6, the vertical velocity in the well hole decreases firstly and increases subsequently, and the horizontal velocity of the first node in the aquifer changes from positive to negative gradually, demonstrating that there exists groundwater exchange between the well hole and the aquifer. The cutoff point of in-flow and out-flow on the well wall is at the half of the well hole in the vertical direction. The flow rate is not even along the well wall, and the farther away from the cutoff point, the larger the flow rate is.

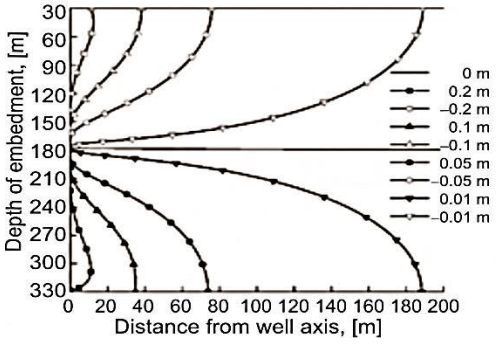

Figure 5. Drawdown contour for SCW

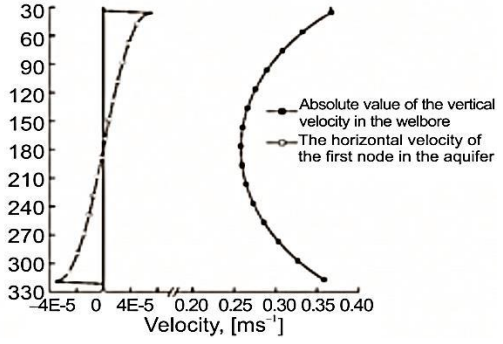

Figure 6. Velocity in the well hole and aquifer *vs.* depth

Figure 7 shows the change of Reynolds number and vertical effective permeability coefficient of well pipe and well hole with depth. As shown in fig. 7, Reynolds number and the vertical effective permeability coefficient is constant along the way when the underground water flow rate keeps unchanged. The groundwater flow rate in the well hole decreases firstly, then increases along the way, so does Reynolds number, correspondingly, the flow changes from the turbulent rough area to the turbulent smooth area, then back to the turbulent rough area. Meanwhile, the effective permeability coefficient increases firstly and decreases afterwards. Variation of the flow rate leads to the change of the resistance, and the effective permeability coefficient changes accordingly. The effective permeability coefficient of the well hole changes in the range of 37-53 ms^{-1}, the roughness of the well hole is larger than that of the well pipe, so the friction coefficient of the well hole is larger, leading to the effective permeability coefficient of the well hole is smaller than that of the well pipe. Nevertheless, the effective permeability coefficient of the well pipe and the well hole are both very large for the flow in them are pipe flow.

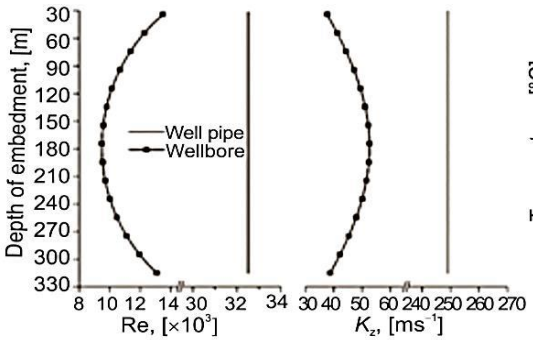

Figure 7. Reynolds number and vertical EHC in drawing pipe and well hole

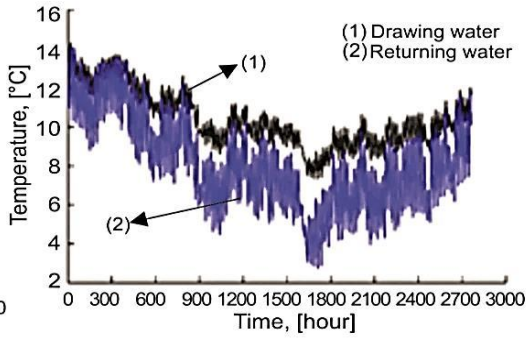

Figure 8. Drawing and returning water temperature of SCW *vs.* time

Figure 8 shows the change of the drawing water temperature and the returning water temperature with time. As shown in fig. 8, temperature of the drawing water and returning water changes drastically, and the drawing water temperature changes with the load. When the load is large, the drawing water temperature is relatively low, this is because the SCW use a bare hole directly, and the flow resistance is larger in the well hole, thus most of the groundwater is circulating in the well pipe, resulting in short circuit of a certain amount of groundwater. During the operation, the maximum drawing water temperature is 14.3 °C and the minimum is 7.4 °C, change of the value is up to 7.0 °C. The temperature of drawing water lower than 9 °C come to 424 hour during the whole region, 15.4% of the total time, this may lead to the low pressure protection parking of the heat pump unit, even freezing of the groundwater. As a result, the ability of the system to respond the sudden load change is limited, and the efficiency of the heat pump unit is also affected to a certain extent. Calculation shows that power consumption of the heat pump unit under the desired adjustment condition is about 8.7% larger than the power consumption when the groundwater temperature keeps unchanged with the initial temperature (power consumption was 97.5 GJ and 89.7 GJ, respectively).

Figure 9 is the isotherm diagram of the aquifer at the end of the heating season. As can be seen from fig. 9, affected area of the SCW is not large with small seepage velocity of groundwater in the aquifer. Calculation results demonstrate that the thermal affected area (defined as the largest radial distance when the temperature difference between the roof and floor of the aquifer is 0.1 °C) is 14.2 m. The temperature changes are concentrated in the upper part of the aquifer, and the temperature is almost constant in the area which is a little far away from the shaft in the lower part of the aquifer. Therefore, the SCW can be relatively close to each other (such as 15 m), not having to worry about the thermal effect between each other.

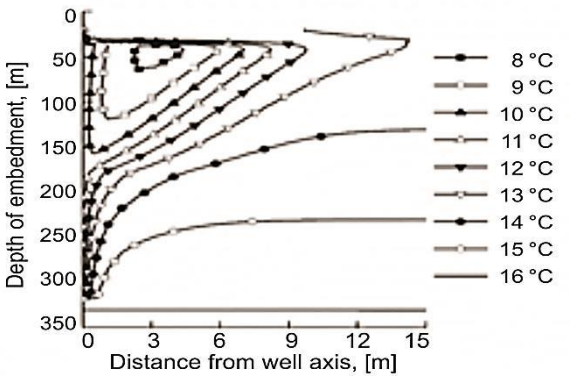

Figure 9. Temperature contour of the aquifer at the end of heating season

Quantitative evaluation of raw water exchange

In the upper part of the SCW, water flows from the well hole to the aquifer, and in the bottom part, water flows from the aquifer to the well hole. The raw water exchange ratio as defined in eq. (3) is used to represent the amount of this part of water. It represents the proportion of water from (or to) the aquifer when drawing or discharging water:

$$ra_{\mathrm{w}} = 1 - \frac{A\left|u_{\mathrm{z,min}}\right|}{V_{\mathrm{w,p}}} \tag{3}$$

where A is the net area of the well hole, equal to the area of the well hole removing the area of the drawing pipe and $u_{\mathrm{z,min}}$ is the minimum vertical velocity in the well hole.

In the heating condition, temperature of the upper part of the well hole is low, and temperature of the lower part of the aquifer is high, thus a certain amount of groundwater flows from the aquifer to the well hole, bringing heat to the SCW, and bears part of the heating load. The load ratio by raw water exchange is used to characterize the magnitude of the aforementioned load, and it indicates the ratio of the load assumed by water exchange to the whole heating load. The load ratio by raw water exchange can be calculated by eq. (4). Here the returning water temperature is taken as the reference temperature:

$$ra_{\mathrm{L}} = -\frac{\int_{z_1}^{z_2} 2\pi r_{\mathrm{h}} C_{\mathrm{w}} u_{\mathrm{r,ha}} (T_{\mathrm{ha}} - T_{\mathrm{r}})\mathrm{d}z}{Q} \times 100\% \tag{4}$$

where ra_{L} is the load ratio by raw water exchange, $u_{\mathrm{r,ha}}$ – the radial flow velocity of groundwater on the interface of the well hole and the aquifer, and the velocity is positive when water flows from the aquifer to the well hole, respectively, T_{ha} – the temperature of the wall of the well, which is the groundwater temperature of inflow and outflow, T_{r} – the temperature of the returning water, Q – the heating load of the SCW, and z_1, z_2 – the starting and ending depth of the well, respectively.

Figure 10 shows the change of the load ratio by raw water exchange with time. As can be seen from fig. 10, the load ratio by raw water exchange of the system is unchanged basically. For this example, the average value of the load ratio by raw water exchange is 23.4%. That is to say, the mass exchange of groundwater between the well hole and the aquifer bears 23.4% of the heating load.

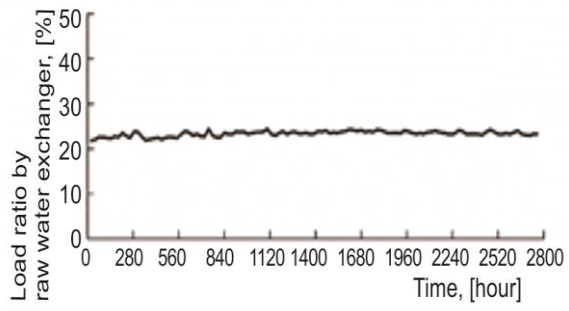

Figure 10. Load ratio by raw water exchange in SCW

Because of the existence of raw water exchange, the heat exchange efficiency of the SCW is much higher than that of the underground heat exchanger of the GSHP, and the ability to bear load has also been improved significantly. Calculation re-sults show that, when the underground rock layer of the SCW is not permeable, the returning water temperature drops below 0 °C after the heat pump operates for 100 hour, and makes the system fail to provide the required load. As shown in tab. 5, with the decrease of permeability coefficient of the aquifer, the raw water exchange ratio and load ratio by raw water exchanged decreases significantly, resulting in the rapid decrease of the drawing

water temperature, and heat transfixion becomes more serious. The raw water exchange ratio is determined by the relative magnitude of the flow resistance in the well hole and the seepage resistance in the aquifer, so it is related to the permeability coefficient of the aquifer and the roughness of the well hole closely.

Table 5. The raw water exchange and drawing water temperature

Permeability coefficient	Raw water exchange ratio	Load ratio by raw water exchange	Mean temperature of drawing water	Minimum temperature of drawing water
ms^{-1}	%	%	°C	°C
$1\cdot10^{-4}$	64.0	49.6	14.2	13.3
$2\cdot10^{-5}$	29.6	23.4	10.4	7.4
$1\cdot10^{-6}$	2.5	2.3	–6.5	–18.5
0	0	0	–10.8	–25.4

Conclusions

The paper established a mathematic model, which was verified by field test of a SCW, of groundwater flow in the SCW and coupled heat transfer of well pipe, well-hole and aquifer. Based on the simulations and experiments, such conclusions could be drawn.

- The thermal dispersion impact must be considered in the heat transfer of the aquifer.
- Simulated values of the drawing water temperature are in good agreement with the measured values under both refrigeration and heating conditions. The error is within 10%.
- In the numerical simulation of a SCW, the parameter sensitivity analysis shows that the output is most sensitive to the water permeability coefficient and heat dispersion of the aquifer, especially the heat dispersion.
- Simulation results show the phenomenon of raw water exchange between the well hole and aquifer clearly. For a typical example, the ratio of raw water exchange in the SCW is 29.6%, and the load ratio by raw water exchange is 23.4%, not changing with time nearly.
- Thermal influence of the SCW to the aquifer is not large (14 m), therefore, distance between two wells can be small.

Acknowledgment

This work was supported by the National Key R&D Program of China for the 13th Five-Year Plan (No. 2017YFC0702600)

Nomenclature

A – net area of the wellbore, [m^2]
B – thickness of the aquifer, [m]
C – volumetric heat capacity, [$kJm^{-3}k^{-1}$]
EHC – equivalent hydraulic conductivity, [ms^{-1}]
K – permeability coefficient, [ms^{-1}]
k – thermal conductivity, [$Wm^{-1}k^{-1}$]
Q – heating load of the SCW, [kW]
q – seepage velocity, [ms^{-1}]
Re – Reynolds number, [–]
r – radius, [m]
T – temperature, [K]
u – flowing velocity of groundwater, [ms^{-1}]
V – water flow rate of the SCW, [m^3s^{-1}]

Greek symbols

α – thermal dispersion, [m]
Δ – difference, [–]

Subscripts

d – drawing pipe
h – well hole
ha – interface between well bore and aquifer
L – load
p – well pipe
ph – interface between well pipe and wellbore
R – returning pipe

r – horizontal direction
w – water
z – vertical direction

References

[1] Yuill, G. K., Mikler, V., Analysis of the Effect of Induced Groundwater Flow on Heat Transfer from a Vertical Open-Hole Concentric-Tube Thermal Well, *ASHRAE Transactions, 101* (1995), 1, pp. 173-185
[2] Minea, V., Experimental Investigation of the Reliability of Residential Standing Column Heat Pump Systems without Bleed in Cold Climates, *Applied Thermal Engineering, 52* (2013), 1, pp. 230-243
[3] Cho, J. H., *et al.*, Performance and Feasibility Study of a Standing Column Well (SCW) System Using a Deep Geothermal Well. *Energy, 9* (2016), 2, pp. 108-113
[4] Tan, C., Kush, E., Semi-Closed Standing Column Well Groundwater Source Heat Pump, *GHPC*, R&D Projec Profile No. 3, 1986, www.geoexchange.org
[5] Woods, K., Ortega, A., The Thermal Response of an Infinite Line of Open Loop Wells for Ground Coupled Heat Pump Systems, *International Journal of Heat and Mass Transfer, 54* (2011), 25-26, pp. 5574-5587
[6] Choi, H. K., *et al.*, Characteristic Analysis of Bleeding Effect on Standing Column Well (SCW) Type Geothermal Heat Exchanger, *Journal of Central South University, 19* (2012), 11, pp. 3202-3207
[7] Lee, C., *et al*., Thermal Performance Analysis of the Standing-Column-Well (SCW) Geothermal Heat Exchanger, *AASCIT Journal of Energy, 2* (2015), Apr., pp. 29-35
[8] Jeon, J. S., *et al*., Applicability of Thermal Response Tests in Designing Standing Column Well System: A Numerical Study, *Energy, 109* (2016), Aug., pp. 679-693
[9] Nguyen, A., *et al*., Influence of Groundwater Flow in Fractured Aquifers on Standing Column Wells Performance, *Geothermics, 58* (2015), Nov., pp. 39-48
[10] Wang, S. Q., *et al*., Variation Characteristics of Aquifer Parameters Induced by Groundwater Source Heat Pump Operation Under Variable Flow, *Journal of Central South University of Technology, 18* (2011), 4, pp. 1272-1277
[11] Ni, L., Operation Performance Research on Heat Source/Sink Well of Groundwater Heat Pump with Pumping & Recharging in the Same Well, Ph. D. thesis, Harbin Institute of Technology, Harbin, China, 2007
[12] Testu, A., *et al*.,Thermal Dispersion for Water or Air Flow through a Bed of Glass Beads, *International Journal of Heat and Mass Transfer, 50* (2007), 7-8, pp. 1469-1484
[13] Deleglise, M., *et al*., Determination of the Thermal Dispersion Coefficient during Radial Filling of a Porous Medium, *Journal of Heat Transfer, 125* (2003), 5, pp. 875-880
[14] Xue, Y., *et al*., Aquifer Thermal Energy Storage: A Numerical Simulation of Field Experiments in China, *Water Resources Research, 26* (1990), 10, pp. 2365-2375
[15] Orio, C. D., *et al.*, A Survey of Standing Column Well Installations in North America, *ASHRAE Transactions, 111* (2005), Part 2, pp. 109-121

Paper submitted: November 10, 2017
Paper revised: November 26, 2017
Paper accepted: November 27, 2017